

Schwinger pair production in AdS_2

B. Pioline♣♠ and J. Troost♠

♣ *LPTHE, Unité mixte du CNRS et des Universités Paris 6 et 7, boîte 126,
4 place Jussieu, 75252 Paris cedex 05, France*

♠ *LPTENS, Unité mixte du CNRS et de l'Ecole Normale Supérieure, Département de
Physique de l'ENS, 24 rue Lhomond, 75231 Paris cedex 05, France*

E-mail: `pioline@lpthe.jussieu.fr`, `troost@lpt.ens.fr`

ABSTRACT: We analyze the pair production of charged particles in two-dimensional Anti-de Sitter space (AdS_2) with a constant, uniform electric field. We compute the production rate both at a semi-classical level, viewing Schwinger pair production as a tunneling event, and at the full quantum level, by extracting the imaginary part of the one-loop amplitude. In contrast to the usual Schwinger pair production in flat space, pair production in AdS_2 requires a sufficiently large electric field $E^2 > M^2 + 1/4$ in order to overcome the confining effect of the AdS geometry – put in another way, the presence of an electric field E raises the Breitenlohner-Freedman bound to $M^2 > -1/4 + E^2$. For E greater than this threshold, the vacuum is unstable to production of charged pairs in the bulk. We expect our results to be helpful in constructing supersymmetric $AdS_2 \times S^2$ perturbative string vacua, which enter in the near-horizon limit of extremal charged black holes. Although the generalized Breitenlohner-Freedman bound is obeyed in these cases, production of BPS particles at threshold is possible and relevant for AdS_2 fragmentation.

Contents

1. Introduction	1
2. Semi-classics of a charged particle in AdS_2	3
2.1 Classical trajectories of a charged particle in AdS_2	3
2.2 Spectrum generating $Sl(2, \mathbb{R})$ symmetry	5
2.3 Tunneling and semi-classical Schwinger pair production	6
2.4 Periodic trajectories and mini-superspace path integral	8
3. One-loop vacuum amplitude in quantum field theory	10
3.1 One-loop amplitude on H_2	11
3.2 Analytic continuation to AdS_2	12
3.3 Spin 1/2 case	15
4. Summary and Discussion	16
A. Zeta function regularisation	19
B. Gravitational back-reaction	21

1. Introduction

Two-dimensional anti-de Sitter space AdS_2 plays a central rôle in the physics of extremal four-dimensional Reissner-Nordström black holes. In Einstein-Maxwell gravity, the near-horizon geometry of an extremal dyonic black hole reduces to the Bertotti-Robinson space-time $AdS_2 \times S^2$ [1], each factor supporting an electric (resp. magnetic) flux proportional to the electric (resp. magnetic) charge of the black hole. In type IIA (IIB) string theory, the same space-time, tensored with a Calabi-Yau three-fold Y of fixed complex (Kähler) structure, appears as the universal near-horizon geometry for all “three-charge” supersymmetric black holes [2, 3]. In the non-extremal case, the near-horizon geometry is still locally $AdS_2 \times S^2$, although the global structure differs [4, 5, 6].

Since the macroscopic entropy of the black hole is proportional to the area of the sphere S^2 , it is natural to expect that a better understanding of string theory in $AdS_2 \times S^2$ may shed light on the microscopic degrees of freedom of extremal black holes. Indeed, the superconformal quantum mechanics of charged D0-branes on $AdS_2 \times S^2$ has been recently shown to reproduce the entropy of a class of extremal black holes [7]. Unfortunately, the study of string theory in the relevant backgrounds is hampered by the existence of Ramond fluxes (see however [8] for recent progress).

It is therefore interesting to note that $AdS_2 \times S^2$ admits an exact conformal field theory description as an asymmetric coset $[SU(2) \times SU(2)]/U(1) \times U(1)$ [9, 10]. The latter can be embedded both in the heterotic string, where the electromagnetic flux is provided by the 10-dimensional gauge fields, or in the type II string, so long as the fluxes originate from the Neveu-Schwarz sector. In particular, the analogue of charged D0-brane probes now are perturbative string states, which can be analyzed by ordinary field theoretic methods. Unfortunately, this conformal field theory remains little understood, as it involves a coset by an hyperbolic generator (see [11] for a recent discussion).

In addition to these technical difficulties, quantum gravity on AdS_2 raises more general puzzles, which have thwarted a direct application of the holographic ideas [12, 13] (see [14, 15, 16] for recent progress). In contrast to higher-dimensional anti-de Sitter space, global AdS_2 has two disconnected time-like boundaries, much like the worldsheet of an ordinary open string. Indeed, global AdS_2 can be viewed as the $SU(2, \mathbb{R})$ invariant ground state of two-dimensional (Liouville) gravity on the strip [17]. Just like perturbative open strings are liable to splitting and joining, AdS_2 can fragment, or rather nucleate baby universes [4]. Such branching geometries can be understood as the near-horizon limit of a multi-centered configuration of supersymmetric RN black holes and form a large moduli space of zero-energy configurations [19]. The fragmentation process can be described by an Euclidean wormhole configuration describing the semi-classical tunneling from one AdS_2 throat of charge $Q_0 > 0$ to two throats of charges $(Q_1 > 0, Q_2 = Q_0 - Q_1 > 0)$ [18]. Interestingly, the production rate turns out to be proportional to the difference of the Hawking entropies of the initial and final state.

When the charge of one black hole is much smaller compared to the others, the process of fragmentation can be understood as the Schwinger pair creation of D0-branes, charged under the electric flux threading AdS_2 . The semi-classical computation has been outlined in the BPS case in [4], producing agreement with the large charge case above. In this work, we give a careful analysis of the one-loop vacuum amplitude for charged particles in AdS_2 in the presence of a constant, uniform electric field. Our computation is closely related, but differs by the type of analytic continuation used, to the computation of the one-loop amplitude for a charged particle in the planar patch of dS_2 performed long ago in [20]. As usual, the real part of the one-loop amplitude carries information about dispersive effects, while the imaginary part gives the (tree-level) production rate for charged particles in the electric field. The latter is expected to vanish in supersymmetric backgrounds, except for BPS states which may be produced abundantly and can have a large gravitational backreaction, leading to the possibility of baby universe formation.

The outline of this paper is as follows. In Section 2 we discuss some aspects of propagation of a charged particle in AdS_2 , give a semi-classical picture of Schwinger pair creation, as a tunneling process in the potential governing the radial motion, and perform a “mini-superspace” computation of the one-loop amplitude. In Section 3, we compute the one-loop vacuum amplitude by analytic continuation from the Landau problem on the hyperbolic plane H_2 . Section 4 contains a Summary and Discussion. An alternative regularization scheme is outlined in Appendix A, and gravitational corrections are discussed in Appendix B.

2. Semi-classics of a charged particle in AdS_2

In this section, we discuss some semi-classical aspects of the propagation of a charged particle in AdS_2 , in the presence of a constant electric field. In Poincaré coordinates, the space-time metric reads

$$ds^2 = a^2 \frac{-dt^2 + dy^2}{y^2} \quad (2.1)$$

where the dimensionful parameter a sets the scale of the curvature, $R = -2/a^2$ (check sign), and the coordinate y is restricted to positive values only. While the locus $y = 0$ corresponds to the boundary of AdS^2 , the geometry can be continued across light-like infinity in the (t, y) plane by defining “strip” coordinates

$$\tau = \arctan(y + t) - \arctan(y - t), \quad \sigma = \arctan(y + t) + \arctan(y - t) \quad (2.2)$$

so that the strip $0 \leq \sigma \leq \pi, \tau \in \mathbb{R}$ now cover the global AdS_2 geometry, with metric

$$ds^2 = a^2 \frac{-d\tau^2 + d\sigma^2}{\sin^2 \sigma} \quad (2.3)$$

In particular, the locus $y = 0$ describes the time-like boundary at $\sigma = 0$ for a finite global time $-\pi \leq \tau \leq \pi$, while $y \rightarrow \infty$ barely touches the other boundary at $\sigma = \pi$ at global time $\tau = 0$. The global geometry of AdS_2 can be covered by two infinite family of Poincaré patches.

2.1 Classical trajectories of a charged particle in AdS_2

Let us now introduce a constant electric field $F = E\omega/a^2$ proportional to the volume element, $\omega = a^2 dt dy / y^2 = a^2 d\tau d\sigma / \sin^2 \sigma$. It is convenient to choose different gauges in the Poincaré and global coordinates,

$$A = E \frac{dt}{y}, \quad \tilde{A} = E \frac{d\tau}{\tan \sigma} \quad (2.4)$$

which differ by a gauge transformation,

$$A - \tilde{A} = Ed\lambda, \quad \lambda = \frac{1}{2} \log \frac{1 + (t + y)^2}{1 + (t - y)^2} = \log \frac{\cos[(\tau - \sigma)/2]}{\cos[(\tau + \sigma)/2]} \quad (2.5)$$

A charged particle propagating in the Poincaré patch of AdS_2 in the presence of an electric field is thus described by the action

$$S[y, t] = \int ds \left\{ \frac{a^2}{2\rho y^2} \left[- \left(\frac{dt}{ds} \right)^2 + \left(\frac{dy}{ds} \right)^2 \right] + \frac{E}{y} \frac{dt}{ds} - \rho \frac{M^2}{2} \right\} \quad (2.6)$$

where the Lagrange multiplier ρ enforces the mass-shell condition. Setting $\rho = 1$, the world-line Hamiltonian becomes

$$H_{\text{Poinc}} = \frac{y^2}{a^2} \left[p_y^2 - \left(p_t - \frac{E}{y} \right)^2 \right] + M^2 \equiv 0 \quad (2.7)$$

and is required to vanish due to reparameterization invariance. In this expression, the momenta canonically conjugate to y, t are given by

$$p_y = \frac{a^2 dy}{y^2 ds}, \quad p_t = -\frac{a^2 dt}{y^2 ds} + \frac{E}{y}. \quad (2.8)$$

Since p_t is a conserved quantity (the Poincaré energy), the motion in the radial coordinate y is simply governed by a one-dimensional potential $V(y)$,

$$p_y^2 + V(y) = 0, \quad V(y) = \frac{M^2}{a^2 y^2} - \left(p_t - \frac{E}{y}\right)^2 \quad (2.9)$$

From now on, we will set the dimensionful parameter $a = 1$. From this expression, it is easy to infer the following facts (see Figure 1):

- i) For small electric field $E^2 < M^2$, the charged particle (electron, for short) stays at a finite distance $y \geq (E + \epsilon M)/p_t$ from the boundary, where $\epsilon = \pm 1$ denotes the sign of p_t , and reaches the horizon of the Poincaré patch at $y = \infty$.
- ii) For large electric field $E^2 > M^2$ and $E p_t > 0$, the motion consists of two branches: one staying at a finite distance $y \geq (E + \epsilon M)/p_t$ from the boundary and reaching the horizon, corresponding to the motion of the electron, and the other, confined near the boundary at $y < (E - \epsilon M)/p_t$, corresponding to the motion of the positron, being emitted and reabsorbed by the boundary of AdS_2 . As we shall explain in Section 2.3, tunneling between these two branches corresponds to Schwinger pair production in the bulk of AdS_2 .
- iii) For large electric field $E^2 > M^2$ and $E p_t < 0$, the motion covers the entire half axis $y > 0$, and consists of two branches extending from the boundary to the bulk, and conversely. These trajectories can be viewed as emission/absorption of an electron from the boundary of AdS_2 .
- iv) For a critical electric field $E^2 = M^2$, the positron trajectory in case ii) disappears into the boundary, while the electron trajectory in case iii) is tangent to the boundary. This case is relevant for BPS particles in a supersymmetric AdS_2 background.

Similarly, in global coordinates, the motion along the spatial direction σ is governed by the potential

$$H_{\text{glob}} = \sin^2 \sigma [p_\sigma^2 + V(\sigma)] \equiv 0, \quad V(\sigma) = \frac{M^2}{\sin^2 \sigma} - \left(p_\tau - \frac{E}{\tan \sigma}\right)^2 \quad (2.10)$$

where the canonical momenta are given by

$$p_\sigma = \frac{a^2 d\sigma}{\sin^2 \sigma ds}, \quad p_\tau = -\frac{a^2 d\tau}{\sin^2 \sigma ds} + \frac{E}{\tan \sigma} \quad (2.11)$$

It is now easy to determine the semi-classical spectrum (see Figure 2) for a fixed value of the global energy p_τ :

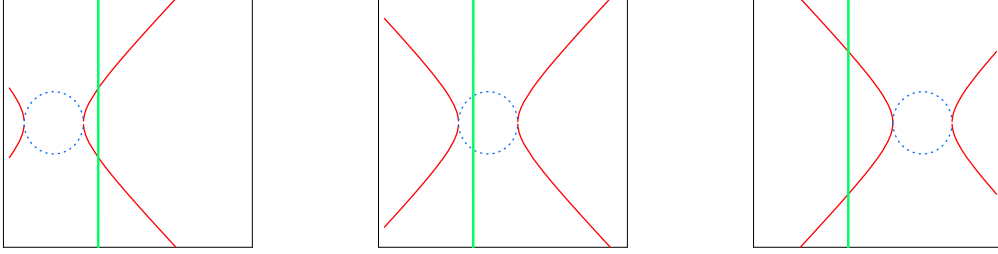


Figure 1: Classical trajectories of a charged particle in the Poincaré patch of AdS_2 . The latter lies to the right of the green line $y = 0$. The solid red (resp. dotted blue) line shows trajectories in real (resp. imaginary) proper time. The right (resp. left) branch corresponds to the electron (resp. positron) trajectory. For weak electric field $E^2 < M^2$ (*center*), the vacuum is stable. For strong electric field $E^2 > M^2$, particles with $Ep_t > 0$ can be pair produced in the bulk (*right*), unlike those with $Ep_t < 0$ (*left*).

- i) For small electric field $E^2 < M^2$, the electron (or the positron) is confined into the bulk of AdS_2 . The semi-classical spectrum can be obtained by the Bohr-Sommerfeld quantization rule (generalizing the analysis for zero electric field in [21]), and consists of discrete states of energy

$$|p_\tau| = \sqrt{M^2 - E^2} + n + \frac{1}{2} \quad (2.12)$$

where n is a non-negative integer.

- ii) When the electric field becomes greater than the critical value $E^2 > M^2$, the potential barriers at $\sigma = 0, \pi$ which prevented the particle to reach the boundaries become potential wells, while a potential barrier appears at finite value of σ . The particle is now confined to either of the two boundaries, and quantum tunneling under the barrier can be interpreted as Schwinger pair creation in the bulk.

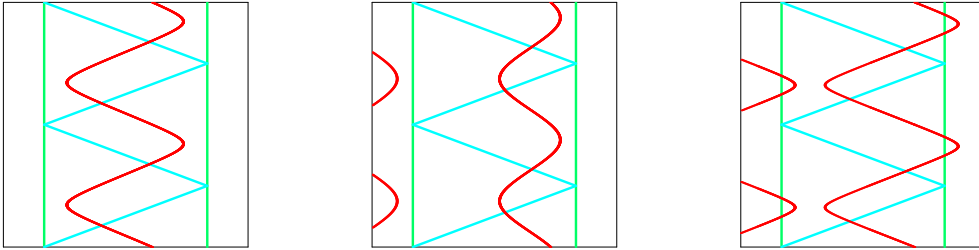


Figure 2: Classical trajectories of a charged particle in global AdS_2 . Green lines denote the boundaries $\sigma = 0, \pi$, blue lines the horizon of the Poincaré patch, and red lines show trajectories in real proper time. The electric field is increased from $E = 0$ (on the left) to $E^2 > M^2 + \frac{1}{4}$ (on the right).

2.2 Spectrum generating $Sl(2, \mathbb{R})$ symmetry

In order to gain further insight on these trajectories, it is useful to note that the Hamiltonians (2.9),(2.10) exhibit an $Sl(2, \mathbb{R})$ symmetry, as a consequence of the isometries of AdS_2 .

In Poincaré coordinates, the canonical generators are

$$L_0 = t p_t + y p_y \quad (2.13)$$

$$L_+ = i p_t \quad (2.14)$$

$$L_- = i \left[(t^2 + y^2) p_t + 2 t y p_y - 2 E y \right] \quad (2.15)$$

while, in global coordinates,

$$L_0 = -i(\cos \tau \sin \sigma \partial_\sigma + \cos \sigma \sin \tau \partial_\tau) + E \sin \sigma \sin \tau \quad (2.16)$$

$$L_+ = -\sin \sigma \sin \tau \partial_\sigma + (1 + \cos \sigma \cos \tau) \partial_\tau + i E \sin \sigma \cos \tau \quad (2.17)$$

$$L_- = \sin \sigma \sin \tau \partial_\sigma + (1 - \cos \sigma \cos \tau) \partial_\tau - i E \sin \sigma \cos \tau \quad (2.18)$$

In either case, the Hamiltonian is related to the quadratic Casimir¹ of the $Sl(2)$ representation via

$$C = -L_0^2 - \frac{1}{2} (L_+ L_- + L_- L_+) = M^2 - E^2 \quad (2.19)$$

Notice in particular that the Poincaré energy $p_t = -iL_+$ and global energy $p_\tau = -i(L_+ + L_-)/2$ correspond to parabolic and elliptic generators, respectively. From our semi-classical discussion in the previous section, we find that the spectrum consists of discrete representations of $Sl(2, \mathbb{R})$ for states below the pair production threshold $E^2 < M^2$, and continuous representations for states above.

Eliminating the momenta p_t, p_y from the three equations (2.13), one readily obtains the equation for the intrinsic trajectory of a charged particle in Poincaré coordinates,

$$\left(y + \frac{E}{iL_+} \right)^2 - \left(t - \frac{L_0}{L_+} \right)^2 = \frac{M^2}{L_+^2} \quad (2.20)$$

Thus, charged particles follow a branch of hyperbola in the Poincaré patch, centered at a radial distance $y = -E/p_t$. This generalizes to the Lorentzian, charged case the well-known fact that (neutral) geodesics on the hyperbolic plane are circles centered on the boundary at $y = 0$. Similarly, the intrinsic trajectory in global coordinates can be obtained by eliminating p_τ, p_σ from (2.16):

$$i(L_+ - L_-) \cos \tau + 2L_0 \sin \tau = 2E \sin \sigma - i(L_+ + L_-) \cos \sigma \quad (2.21)$$

Notice in particular that all trajectories have the same period 2π in global time τ .

2.3 Tunneling and semi-classical Schwinger pair production

As first discussed in [22], and reviewed e.g. in [23], Schwinger pair production can be understood semi-classically as a tunneling process between two classically allowed regions of the potential describing the relativistic motion of the electron in the presence of an electric field. For example, in two-dimensional Minkowski space with a constant electric

¹Although Eqs (2.13),(2.16) are classical, their quantum counterpart is simply obtained by replacing the momenta p_i by $-i\partial_i$, preserving the ordering shown; as a result, the resulting quadratic Casimir is shifted to $C = M^2 - E^2 + \frac{1}{4}$, and M^2 is shifted to $M^2 + \frac{1}{4}$.

field E , the motion along the spatial coordinate x , at fixed energy p_t , is given by the inverted harmonic potential

$$p_x^2 + V(x) = 0, \quad V(x) = M^2 - (p_t - Ex)^2 \quad (2.22)$$

Particles to the right of the potential barrier at $x = p_t/E$ correspond to electrons, while particles to the left are positrons. Tunneling under the barrier corresponds to a stimulated emission of positron-electron pairs. The tunneling rate can be computed semi-classically by evolving the wave function in imaginary proper time, which amounts to flipping the sign of the potential. There is now an Euclidean trajectory relating the two turning points, with classical action

$$S_{cl} = \int_{(p_t-M)/E}^{(p_t+M)/E} \sqrt{V(x)} dx = \frac{\pi M^2}{2E} \quad (2.23)$$

The semi-classical pair creation rate, either for stimulated or spontaneous processes, is therefore given by $\exp(-2S_{cl})$, in agreement with Schwinger's classic result. Notice that the Euclidean instanton can be viewed as the motion of a charged particle in a constant *magnetic* field during a Larmor period.

By the same token, the pair production rate in AdS_2 may be computed semi-classically by evaluating the action of the instanton which controls the tunneling between the electron and positron branches, in the case (ii) above. As in flat space, the propagation of a charged particle on AdS_2 in imaginary proper time amounts to a real-time evolution under the Hamiltonian

$$H_B = \frac{y^2}{a^2} \left[p_y^2 + \left(p_x - \frac{E}{y} \right)^2 \right] \quad (2.24)$$

upon identifying $B = E, H_B \equiv M^2$. Formula (2.24) is now the Hamiltonian of a charged particle on the Euclidean hyperbolic plane H_2 , with metric and magnetic field

$$ds^2 = a^2 \frac{dx^2 + dy^2}{y^2}, \quad A = B \frac{dx}{y} \quad (2.25)$$

The Landau problem on H_2 was discussed in detail in [24] (see also e.g. [25, 26]), with the following semi-classical results:

- a) Classical trajectories are circles in the (x, y) plane, centered at $y = B/p_x$. For small magnetic field $B^2 < H$, they are open trajectories which intersect the boundary $y = 0$; for large magnetic field $B^2 > H \geq 0$, they are closed trajectories in the bulk of H_2 .
- b) Open trajectories reach the boundary in infinite proper time, and have an infinite action. They correspond to a continuum of states with energy $H \geq B^2$.
- c) Closed trajectories have a finite action

$$S = \pi \left(B - \sqrt{B^2 - H} \right) \quad (2.26)$$

By the Bohr-Sommerfeld condition, they correspond to a finite number of discrete states with energy²

$$H_n = \left(n + \frac{1}{2}\right) \left(2B - n - \frac{1}{2}\right) \quad (2.27)$$

with $0 < n + 1/2 < B$.

Cases b) and c) are the analytic continuation of the electric trajectories i) and ii). We conclude that Schwinger pair production in the bulk of AdS_2 , corresponding to the tunneling between the two electric trajectories of type ii), is mediated by an instanton trajectory of type c), with rate

$$\Gamma_{bulk} = \exp \left[-2\pi \left(E - \sqrt{E^2 - M^2} \right) \right] \quad (2.28)$$

As we shall see, this semi-classical result agrees with the quantum analysis in Section 3. It is also easy to check that (2.28) is in agreement with the result of [4] for the action of a $(D - 2)$ spherical brane in AdS_D , with $D = 2$.

Finally, let us compare the pair production rates in global AdS_2 and in the Poincaré patch. The WKB actions controlling the tunneling process are given by

$$S_{\text{Poinc.}} = \oint p_y dy, \quad S_{\text{Glob.}} = \oint p_\sigma d\sigma \quad (2.29)$$

where the integral runs over a closed periodic trajectory³ in imaginary time, and $p_y = \sqrt{V(y)}$ (resp. $p_\sigma = \sqrt{V(\sigma)}$) is the momentum derived from the potential $V(y)$ in (2.9) (resp. $V(\sigma)$ in (2.10)) respectively, and $p_y = \sqrt{V(y)}$ (resp. $p_\sigma = \sqrt{V(\sigma)}$). Noting that the Lagrangians in Poincaré and global coordinates differ by a total derivative, we have

$$p_y dy + p_t dt - H_{\text{Poinc.}} ds = p_\sigma d\sigma + p_\tau d\tau - H_{\text{Glob.}} ds + Ed\lambda \quad (2.30)$$

The Hamiltonians $H_{\text{Poinc.}}$ and $H_{\text{Glob.}}$ are equal off-shell, hence cancel from this equality. Let us now integrate (2.30) along a closed Euclidean trajectory: since p_t and p_τ are conserved quantities and their conjugate variables are periodic, we find that only the first term on either side remains, and conclude that the semi-classical tunneling rates are the same in the Poincaré patch and in global AdS_2 . This suggests that the equivalence of the Poincaré and global vacuum demonstrated for neutral particles in [27] carries over to the charged case.

2.4 Periodic trajectories and mini-superspace path integral

Quantum mechanically, the pair creation rate can be obtained as the imaginary part of the one-loop vacuum amplitude of a charged particle in AdS_2 , with action (2.6). Before turning to a quantum field theory computation in Section 3, it is instructive to study a “mini-superspace” version of this computation, following the approach initiated in [28] for monopole pair creation in a magnetic field (see [29] for a review of this technique).

²It is perhaps worth noting that, in contrast to the flat space case, the area enclosed by each trajectory is not a multiple of a fixed quantum, but rather $A_n = \pi \left(n + \frac{1}{2}\right) / \left[B - \frac{1}{2} \left(n + \frac{1}{2}\right)\right]$.

³The standard WKB prescription of integrating over *half* a period would not be gauge-invariant.

Recall that the logarithm of the one-loop vacuum amplitude (or free energy, for brevity) is given by the Euclidean path integral

$$W_B = - \int_0^\infty \frac{d\tilde{\rho}}{\tilde{\rho}} \int [dx(s)] [dy(s)] \exp(-S_E) \quad (2.31)$$

where S_E is the Euclidean action

$$S[x, y, \rho] = \int ds \left\{ \frac{a^2}{2\rho y^2} \left[\left(\frac{dx}{ds} \right)^2 + \left(\frac{dy}{ds} \right)^2 \right] + \frac{B}{y} \frac{dx}{ds} - \rho \frac{M^2}{2} \right\} \quad (2.32)$$

and the path integral is restricted to configurations periodic in imaginary time s with period 2π . For later convenience, we shall use the gauge $\rho(s) = \tilde{\rho}/y(s)$. The idea now is to truncate the path integral to a family of closed off-shell configurations which contain the instantons mediating the pair creation process, namely circles in the cartesian (x, y) plane with arbitrary radius R and center (x_0, y_0) :

$$x(s) = x_0 + R \cos ks, \quad y(s) = y_0 + R \sin ks \quad (2.33)$$

where $k \in \mathbb{Z}$ and $s \in [0, 2\pi]$ parameterizes the closed trajectory. This becomes a solution of the equations of motion when

$$R = M y_0/B, \quad \tilde{\rho} = \frac{y_0 k}{B} \quad (2.34)$$

We now truncate the path integral over $x(s), y(s)$ to the “mini-superspace” of constant values of (R, x_0, y_0) . Using the natural conformal-invariant integration measure, one obtains the mini-superspace approximation to the one-loop path integral,

$$I_{mini} = B^2 \int \frac{dx_0}{y_0^2} \frac{dy_0}{y_0^2} \int_0^\infty \frac{R dR}{y_0^2} \int_0^\infty \frac{d\tilde{\rho}}{\tilde{\rho}} \exp(-S_E) \quad (2.35)$$

where S is the classical Euclidean action of the configuration (2.33) (assuming $0 < R < y_0$)

$$S_E = \int_0^{2\pi} ds \mathcal{L} = \pi \left[\frac{M^2 \tilde{\rho}}{\sqrt{y_0^2 - R^2}} + \frac{k^2 R^2}{\tilde{\rho} \sqrt{y_0^2 - R^2}} + 2 B k \left(1 - \frac{y_0}{\sqrt{y_0^2 - R^2}} \right) \right] \quad (2.36)$$

By conformal invariance, S depends only on the ratio R/y_0 and $\tilde{\rho}/y_0$. The action (2.36) is stationary with respect to the radius R at

$$\langle R \rangle = \frac{1}{k} \sqrt{M^2 \tilde{\rho}^2 - 2 k B y_0 \tilde{\rho} + 2 y_0^2 k^2} \quad (2.37)$$

for any ρ ; the resulting action at this saddle point action becomes

$$S_{\langle R \rangle} = \pi \left(2 k B - \sqrt{\frac{k y_0 (2 B \tilde{\rho} - k y_0)}{\tilde{\rho}^2} - M^2} \right) \quad (2.38)$$

Note in particular that in contrast to the flat space case, the integral over the radius modulus R never leads to a pole in the $\tilde{\rho}$ Schwinger parameter plane.

If instead one first integrates over the Schwinger parameter $\tilde{\rho}$, one finds that S is stationary at $\langle \tilde{\rho} \rangle = kR/M$, with saddle point action

$$S_{\langle \tilde{\rho} \rangle} = \frac{2\pi k}{\sqrt{y_0^2 - R^2}} \left[M R + B \left(-y_0 + \sqrt{y_0^2 - R^2} \right) \right] \quad (2.39)$$

In either case, extremizing (2.39) with respect to R , or (2.38) with respect to $\tilde{\rho}$, the resulting classical action becomes

$$S_{\langle R, \tilde{\rho} \rangle} = 2\pi k \left(B - \sqrt{B^2 - M^2} \right) \quad (2.40)$$

with saddle-point values

$$\langle R \rangle = M \frac{y_0}{B}, \quad \tilde{\rho} = k \frac{y_0}{B} \quad (2.41)$$

in agreement with the on-shell values (2.34). In the one-instanton case $k = 1$, this indeed reproduces the result (2.26) for $k = 1$.

The advantage of this approach is that one can now evaluate the contribution of fluctuations (in the mini-superspace sector) around the saddle point (2.41). Varying the action (2.36) with respect to both (R, ρ) , the one-loop determinant around the Gaussian saddle point is given by

$$\det = - \left[\frac{4\pi}{y_0^2} \frac{B^3 M}{B^2 - M^2} \right]^2 < 0 \quad (2.42)$$

The zero-modes arising from conformal invariance contribute a factor of volume. Assuming that higher fluctuation modes around the “quasi-zero-mode trajectories” (2.33) all have positive eigenvalues, one obtains a negative fluctuation determinant, implying that the saddle point (2.41) indeed contributes to the imaginary part of the one-loop amplitude. Finally, including the summation measure (2.35), one obtains, in the saddle point approximation,

$$I_{mini} \sim i V \frac{B^2 - M^2}{B} \sum_{k=1}^{\infty} \frac{1}{k} \exp \left[-2\pi k \left(E - \sqrt{E^2 - M^2} \right) \right] \quad (2.43)$$

where $V = \int dx_0 dy_0 / y_0^2$ is the regularized volume of AdS_2 . Identifying $B = E$ and taking the limit $B \gg M$, we recover precisely the first term of the exact field theory result (3.25) computed in the next Section (the other term in (3.25) can be seen to arise from quantum corrections around the saddle point).

3. One-loop vacuum amplitude in quantum field theory

Having reached a semi-classical understanding of the pair production process, we now turn to a quantum field theoretical treatment, and evaluate the one-loop vacuum amplitude for a charged, spinless particle in AdS_2 , with particular emphasis on its imaginary part. Following the approach in [20], we start from the Euclidean problem of a charged particle on the hyperbolic plane H_2 , and analytically continue to the Lorentzian problem of interest⁴.

⁴We thus deviate from [20], which deals with a different analytic continuation leading to dS_2 .

3.1 One-loop amplitude on H_2

We have briefly recalled the semi-classics of the Landau problem on the hyperbolic plane in Section (2.3) above. As observed in [24], the semi-classical approximation to the energy spectrum is in fact exact, up to a replacement of the energy H by $H + \frac{1}{4}$. The spectrum of the magnetic Laplacian on H_2

$$H_B = -y^2 [\partial_y^2 + (\partial_x - iB/y)^2] \quad (3.1)$$

consists of a finite number of discrete Landau states, with energy

$$H_n = B^2 + \frac{1}{4} - (B - n - \frac{1}{2})^2 \quad (3.2)$$

where $0 \leq n \leq B - \frac{1}{2}$ is a non-negative integer, and a continuum of delta-normalizable states with energy

$$H_\nu = B^2 + \nu^2 + \frac{1}{4} \quad (3.3)$$

for $\nu \in \mathbb{R}^+$. Discrete states are present only for $B > 1/2$.

Both the discrete states (3.2) and continuous states (3.3) are infinitely degenerate with respect to the quantum number p_t , which takes value in \mathbb{R}^+ for discrete states, and \mathbb{R} for continuous states (we assume $B > 0$ throughout, and set the curvature radius to $a = 1$). This infinite degeneracy can be regularized by introducing an infrared volume cut-off V , leading to a degeneracy

$$\rho_n = \frac{V}{2\pi} \left(B - n - \frac{1}{2} \right) \quad (3.4)$$

for the discrete states, and a density of states

$$\rho_c(\nu) = \frac{V}{2\pi} \frac{\nu \sinh 2\pi\nu}{\cosh 2\pi\nu + \cos 2\pi B} \quad (3.5)$$

in the continuum [20]. This allows us to compute the heat kernel for the magnetic Laplacian (3.1),

$$K_B(\tau) := \text{Tr } e^{-\tau H_B} = \sum_{n=0}^{B-1/2} \rho_n e^{-\tau H_n} + \int_0^\infty d\nu \rho_c(\nu) e^{-\tau H_\nu} \quad (3.6)$$

Using parity considerations as well as the identity

$$\Im \left[\psi \left(\frac{1}{2} + i\nu - B \right) + \psi \left(\frac{1}{2} + i\nu + B \right) \right] = \pi \frac{\sinh 2\pi\nu}{\cosh 2\pi\nu + \cos 2\pi B} \quad (3.7)$$

where $\psi(x) = d \log \Gamma(x)/dx$ is the Euler ψ function, the contribution of the continuum can be rewritten as an integral

$$K_{B;c}(\tau) = \frac{V}{4\pi^2 i} \int_{-\infty}^\infty d\nu \nu \left[\psi \left(\frac{1}{2} + i\nu - B \right) + \psi \left(\frac{1}{2} + i\nu + B \right) \right] e^{-\tau E_\nu}. \quad (3.8)$$

on the complete real axis $\nu \in \mathbb{R}$. Now, observe that the integrand has poles when the argument of $\psi(z)$ is a negative integer, i.e. at:

$$\nu = i \left(n + \frac{1}{2} \pm B \right), \quad n = 0, 1, 2, \dots \quad (3.9)$$

For small $B < 1/2$, all poles lie in the upper half plane (see Figure 3). As B is increased past $n + 1/2$, the pole $i(n + \frac{1}{2} - B)$ crosses over into the lower half plane. It can be checked that the residue at the pole is precisely equal to the contribution of the discrete state of energy E_n . The contributions of the discrete and continuous spectrum may thus be combined by shifting the integration contour in the lower half plane so that it passes below the poles at $\nu = i(n + \frac{1}{2} - B)$ for any $n \geq 0$. The complete heat kernel $K_B(\tau)$ of the magnetic Laplacian may thus be concisely written as

$$K_B(\tau) = \frac{V}{4\pi^2 i} \int_{C=-i(B-\frac{1}{2}+\epsilon)+\mathbb{R}} d\nu \nu \left[\psi \left(\frac{1}{2} + i\nu - B \right) + \psi \left(\frac{1}{2} + i\nu + B \right) \right] e^{-\tau E_\nu}. \quad (3.10)$$

The one-loop vacuum amplitude, or free energy, can now be obtained from the heat kernel by integrating over Schwinger time τ ,

$$W_B = \text{Tr} \log (H_B + M^2) = - \int_0^\infty \frac{d\tau}{\tau} K_B(\tau) e^{-\tau M^2} \quad (3.11)$$

(More precisely, this equation applies to the differences $W_B - W_0$ and $K_B - K_0$).

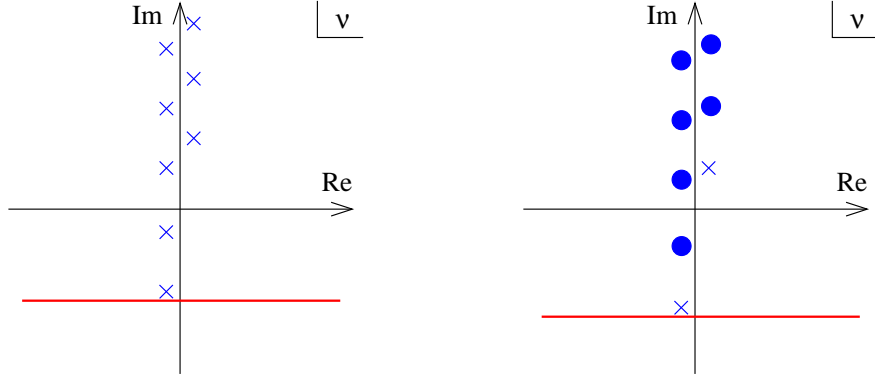


Figure 3: The analytic structure of the heat kernel for the magnetic Laplacian in the ν plane. On the left, the poles and integration contour for the scalar charged particle, on the right for the spin 1/2 particle to be discussed in Section 3.4. The integration contour C (in bold red) sums the contribution of both the discrete and continuous states. The crosses (in blue) denote single poles, the (blue) dots denote double poles. The poles all lie on the imaginary axis, but have been slightly separated for clarity.

3.2 Analytic continuation to AdS_2

After first quantization, the world-line Hamiltonian (2.7) for an electron in (the Poincaré patch of) AdS_2 becomes the Klein-Gordon equation $(H_E + M^2)\phi = 0$ on the complex wave

function $\phi(y, t)$ of the electron, where

$$H_E := -y^2 [\partial_y^2 - (\partial_t - iE/y)^2] \quad (3.12)$$

is the Klein-Gordon operator for a charged field on AdS_2 with a constant electric field. Just as in the magnetic problem, the one-loop amplitude $W_E = \log \det(H_E + M^2)$ can be obtained from the heat kernel by integration with respect to Schwinger time,

$$W_E = - \int_0^\infty \frac{d\tau}{\tau} K_E(\tau) e^{-\tau M^2}, \quad K_E(\tau) := \text{Tr} e^{-\tau H_E} \quad (3.13)$$

While we could in principle construct $K_E(\tau)$ from the density of continuous states in the potential $V(y)$ in (2.9) (or from the density of continuous and discrete states in the potential $V(\sigma)$ in (2.10)), we choose instead to obtain it by analytic continuation of the magnetic heat kernel (3.10).

For this purpose, notice that the Schwinger Hamiltonian (3.12) is turned into the Landau Hamiltonian (3.1) by identifying

$$x = -it, \quad B = iE, \quad H = -M^2 \quad (3.14)$$

Under this analytic continuation, the discrete states (3.2) become states with imaginary mass squared M^2 , and are *not* part of the delta-normalizable spectrum of the Schwinger Hamiltonian (3.12). On the other hand, the continuous states (3.3) of the magnetic problem yield a continuum of states with mass squared below the generalized Breitenlohner-Freedman bound $M^2 < E^2 - \frac{1}{4}$, which are not delta-normalizable near $y = 0$, but are nevertheless part of the physical spectrum, and indeed are responsible for the pair creation process.

In order to obtain the heat kernel $K_E(z)$ for the electric problem, let us start from the magnetic problem (3.10), set $B = e^{i\theta} E$ and increase θ from 0 to $\pi/2$. For $\theta = 0$, the analytic structure of the integrand in the ν plane consists of poles (3.9), a finite number of which lie in the lower half plane. As θ is increased up to $\pi/2$, all the poles migrate to the sunny upper-half ν plane. We can therefore lift the contour C to the real axis, and obtain

$$K_E(\tau) = \frac{V}{4\pi^2 i} \int_{\mathbb{R}} d\nu \nu \left[\psi \left(\frac{1}{2} + i(\nu - E) \right) + \psi \left(\frac{1}{2} + i(\nu + E) \right) \right] e^{-\tau E \nu}. \quad (3.15)$$

Reversing the argument which took us from (3.6) to (3.8), this may be rewritten as an integral over the continuous spectrum of the Klein-Gordon operator (3.12)

$$K_E(\tau) = \int_0^\infty d\nu \rho_E(\nu) e^{-\tau E \nu} \quad (3.16)$$

where the density of states⁵ is now given by

$$\rho_E(\nu) = \frac{V}{2\pi} \frac{\nu \sinh 2\pi\nu}{\cosh 2\pi\nu + \cosh 2\pi E} \quad (3.17)$$

⁵This applies to states with real ν , i.e. below the BF bound $M^2 < E^2 - 1/4$.

The one-loop amplitude is thus given by the integral over the Schwinger parameter τ ,

$$W_E = - \int_0^\infty \frac{d\tau}{\tau} \int_0^\infty d\nu \rho_E(\nu) e^{-\tau(M^2 - E^2 + \nu^2 + \frac{1}{4})} \quad (3.18)$$

For small electric field $E^2 < M^2 + 1/4$, the one-loop amplitude is well defined and real. For large electric field however, the integral over τ has an infrared divergence when $\nu < \Delta$, where $\Delta = \sqrt{E^2 - M^2 - \frac{1}{4}}$. This divergence is analogous to the tachyonic divergence of the bosonic string, and is expected to give an imaginary contribution to the one-loop amplitude. In order to extract the imaginary part, it is convenient to expand the density of states as the difference of geometric series

$$\rho_E(\nu) = \frac{V\nu}{2\pi} \sum_{k=1}^{\infty} (-1)^k \left[e^{-2\pi(E+\nu)k} - e^{-2\pi(E-\nu)k} \right] \quad (3.19)$$

which converge in the region of interest $0 < \nu < \Delta < E$. Using parity considerations once again, the imaginary part of the one-loop amplitude may be written as

$$\Im(W_E) = -\frac{V}{2\pi} \Im \left\{ \sum_{k=1}^{\infty} (-1)^k \int_0^\infty \frac{d\tau}{\tau} \int_{-\Delta}^{\Delta} \nu d\nu \exp \left[-2\pi(E + \nu)k + \tau(\Delta^2 - \nu^2) \right] \right\} \quad (3.20)$$

The imaginary part is not affected by extending the integration range to the full ν axis⁶. The ν integral now becomes Gaussian, and yields

$$\Im(W_E) = \frac{V}{2\pi} \Im \left\{ \sum_{k=1}^{\infty} (-1)^k k \int_0^\infty \frac{d\tau}{\tau} \left(\frac{\pi}{\tau} \right)^{3/2} \exp \left[-2\pi k E + \frac{\pi^2 k^2}{\tau} + \tau \Delta^2 \right] \right\} \quad (3.21)$$

The remaining integral over τ is of Bessel type, however it diverges at both ends of the τ integration range. Generalizing the procedure described in [32] for regularizing divergent integrals, we define it by analytic continuation of the integral

$$\int_0^\infty \frac{d\tau}{\tau^{5/2}} \exp(-a\tau - b/\tau) = \frac{\sqrt{\pi}}{2b^{3/2}} \left(1 + 2\sqrt{ab} \right) e^{-2\sqrt{ab}} \quad (3.22)$$

which is convergent and real for $\Re(a) > 0, \Re(b) > 0$. Analytically continuing⁷ $(a, b) \rightarrow e^{i\pi}(a, b)$, we find a purely imaginary result,

$$\int_0^\infty \frac{d\tau}{\tau^{5/2}} \exp(a\tau + b/\tau) = \frac{i\sqrt{\pi}}{2b^{3/2}} \left(1 - 2\sqrt{ab} \right) e^{2\sqrt{ab}} \quad (3.23)$$

Using this prescription, we obtain

$$\Im(W_E) = \frac{V}{4\pi^2} \sum_{k=1}^{\infty} (-1)^k \frac{1}{k^2} (1 - 2\pi k \Delta) \exp[-2\pi k (E - \Delta)] \quad (3.24)$$

⁶A subtlety with this prescription is that the sum over k will only become convergent after performing the integral over ν .

⁷An alternative prescription would be to rotate a and b oppositely, but the result would not have the correct semi-classical limit.

This provides our final result for the pair production rate of spinless charged particles in AdS_2 ,

$$\Im(W_E) = \frac{V}{4\pi^2} \left[\text{Li}_2 \left(-e^{-2\pi(E-\Delta)} \right) - 2\pi\Delta \text{Li}_1 \left(-e^{-2\pi(E-\Delta)} \right) \right] \quad (3.25)$$

where $\text{Li}_n(x) = \sum_{k=1}^{\infty} x^k/k^n$ is the standard poly-logarithm function, and we recall that $\Delta = \sqrt{E^2 - M^2 - \frac{1}{4}} > 0$. Several comments are in order:

- For large electric field $E \gg M$, the second term dominates over the first. In this limit, the effect of curvature can be neglected. Approximating $\Delta \sim E - M^2/(2E)$, we recover the standard Schwinger result in two flat dimensions,

$$\Im W_E \rightarrow \frac{V}{2\pi} \sum_{k=1}^{\infty} \frac{E}{k} \exp(-\pi k M^2/E) \quad (3.26)$$

- Semi-classically, the result (3.25) shows contributions of saddle points with action $2\pi k(E - \Delta)$: this is precisely the action of the closed periodic orbits of the magnetic problem which control the tunneling under the barrier of the electric problem. Our mini-superspace analysis in Section 2.3 precisely reproduces the logarithmic term in (3.25), which dominates in the semi-classical limit over the dilogarithm.
- The di-logarithm however dominates near the pair production threshold $E^2 \sim M^2 + \frac{1}{4}$, and leads to a finite non-zero result. The imaginary part of the amplitude is therefore discontinuous at the threshold.

3.3 Spin 1/2 case

The case of charged spin 1/2 case can be treated by very similar techniques, using the fact that the square of the Dirac operator is a Klein-Gordon type operator on the tensor product $L_2(AdS_2) \otimes \mathbb{C}^2$. The spectrum in the Euclidean magnetic case has been derived in [20], and consists of a finite number of discrete Landau states, with energy

$$H_{n,1/2} = B^2 - (n - B)^2 \quad (3.27)$$

where $0 \leq n < B$ is a non-negative integer, and a continuum of delta-normalizable states with energy

$$H_{\nu,1/2} = B^2 + \nu^2 \quad (3.28)$$

for $\nu \in \mathbb{R}^+$. All discrete states except for the ground state $n = 0$ are doubly degenerate. In contrast to the spin 0 case, discrete states exist for arbitrarily small B .

The density of states of the continuous series can be found in [20]

$$\rho_{E,1/2}(\nu) = \frac{V\nu}{\pi} \frac{\sinh 2\pi\nu}{\cosh 2\pi\nu - \cosh 2\pi E} \quad (3.29)$$

and rewritten in the same way as in (3.7),

$$\rho_{E,1/2}(\nu) = \frac{V\nu}{\pi^2} \Im [\psi(i\nu - B) + \psi(i\nu - B + 1) + \psi(i\nu + B) + \psi(i\nu + B + 1)] \quad (3.30)$$

Again, the contributions of the discrete states to the heat kernel or zeta function can be absorbed by shifting the contour C so that it lies below all the poles in the lower ν plane. Under analytic continuation to the electric case, all poles move into the upper half plane as in the spinless case. The imaginary part of the free energy can be computed by expanding the density of states as a sum of two convergent geometric series,

$$\rho_{E,1/2}(\nu) = \frac{V\nu}{\pi} \sum_{k=1}^{\infty} \left[e^{-2\pi(E+\nu)k} - e^{-2\pi(E-\nu)k} \right] \quad (3.31)$$

We state the final result,

$$\Im W_E = \frac{V}{2\pi^2} \left[\text{Li}_2 \left(e^{-2\pi(E-\Delta_{1/2})} \right) - 2\pi\Delta_{1/2} \text{Li}_1 \left(e^{-2\pi(E-\Delta_{1/2})} \right) \right] \quad (3.32)$$

where $\Delta_{1/2} = \sqrt{E^2 - M^2}$. As in flat space, we observe that the order k instanton terms all come with the same sign, in contrast with the bosonic (spinless) case.

4. Summary and Discussion

In this work, we have performed a detailed analysis of the quantum fluctuations of charged particles in AdS_2 , both at a semi-classical and field-theoretic level, with a particular emphasis on the production of charged pairs by the Schwinger mechanism. Let us recapitulate the main points of our analysis, with a few more remarks:

- Due to the confining property of the AdS geometry, pair production only takes place when the electric field exceeds the threshold $E^2 > M^2 + 1/4$. This is in contrast to flat space [31], where pair production occurs (albeit non-perturbatively in E) for arbitrarily small electric field, which consequently relaxes to zero. This property is crucial for the existence of stable supersymmetric $AdS_2 \times S^2$ vacua, as occur near the horizon of extremal Reissner-Nordström black holes.
- One way of rephrasing this property is that the standard Breitenlohner-Freedman bound $M^2 \geq -1/4$ for a neutral particle in AdS_2 [30] is raised in the presence of an electric field E to

$$M^2 \geq -\frac{1}{4} + E^2 \quad (4.1)$$

This is simply the normalizability condition for the wave function of a charged particle in the Poincaré patch near the boundary $y = 0$ of AdS_2 . Pair production takes place at large electric field when this condition is no longer met, and is qualitatively similar to tachyon condensation. This phenomenon will be generic for AdS -spaces with a flux proportional to the volume, in the presence of branes coupling to the flux, although a simple field theory approach may no longer be applicable.

- As in flat space, pair production takes place via tunneling in the potential governing the radial motion. It is thus governed by the Euclidean trajectory of a charged

particle on the hyperbolic plane H_2 with a constant magnetic field. The production rate in the Poincaré patch is given semi-classically by

$$\Gamma \sim \exp \left[-2\pi \left(E - \sqrt{E^2 - M^2 - \frac{1}{4}} \right) \right] \quad (4.2)$$

and reduces to the flat space answer $\exp(-M^2/(2E))$ when the ratio $(M^2 + (1/4))/E^2$ becomes small.

- The above observations are confirmed by a detailed analysis of the one-loop amplitude W_E . In contrast to the flat space case, the imaginary part of W_E does *not* receive contributions from poles of the heat kernel in the imaginary Schwinger time domain, but rather from unstable saddle points. This can be seen in the mini-superspace version of the one-loop integral, which shows that the quadratic action around Euclidean periodic trajectories has no zero-modes, but has one unstable mode.
- Our result for the imaginary part of the one-loop amplitude assumes a specific choice of vacuum. Due to existence of time-like boundaries, it is also necessary to specify boundary conditions for light particles which can escape to the boundary or be injected from it. In Appendix A, we propose a different regularization scheme which leads to a different imaginary part, with two saddle points interfering destructively at threshold. It would be desirable to understand the vacuum and boundary conditions implicit in both cases in detail.
- We have shown that the semi-classical tunneling rates agree in the Poincaré patch and in global AdS_2 . While we expect that the known equality of the Poincaré and global vacua for neutral particles carries over to the charged case, it would be interesting to confirm this by constructing the one-loop amplitude in global AdS_2 .
- Our computation has neglected gravitational backreaction. The latter has been discussed long ago using an Euclidean approach to quantum gravity [35]. While their results are in agreement with ours at leading order in Newton's constant G (see Appendix B), they indicate that the tunneling action is corrected by gravitational effects to

$$S = 2\pi(E - \sqrt{E^2 - M^2}) + \frac{\pi G}{2} E \left(-2E + \frac{2E^2 - M^2}{\sqrt{E^2 - M^2}} \right) \quad (4.3)$$

(with $E > 0$) at first order in G . In particular, they seem to indicate that the threshold for particle creation is further raised to $|E| > M + GM^2/4$.

- As already stated, pair production is not expected to take place in a supersymmetric setting. Nevertheless, there may exist charged BPS states which just saturate the generalized Breitenlohner-Freedman bound (4.1). This is in particular so when AdS_2 arises as the near horizon geometry of a large number of BPS branes: an extra brane probe of the same type as those which created the background will saturate the BPS bound (4.1). Such states may be abundantly produced and will cause AdS to

fragment in several baby universes [4]. While the semi-classical production rate has been computed in [4], it is important to note that restricting to the leading term in the semi-classical approximation is inappropriate at the threshold for pair production, where the quantum corrections due to the dilogarithms in (3.25) become dominant. It is also important to specify the spectrum and boundary conditions, as the results (3.25) and (A.12) lead to very different physics at threshold.

- We expect our results to be useful in understanding perturbative (heterotic or type II) string theory on $AdS_2 \times S^2$. As pointed out in [11], the partition function of string theory on the hyperbolic deformation $Sl(2)/U(1)_k$ has remained elusive, as it requires an understanding of characters of $Sl(2)/U(1)_k$ in an hyperbolic basis. Using the results in the present work, appropriately generalized to higher spins, it should be possible to take a constructive approach to this problem and get at the string one-loop amplitude by summing the one-loop vacuum amplitude of each state in the spectrum.
- Charged particles in AdS_2 also arise in the context of open strings stretched between two D-branes in AdS_3 ⁸. Recall that AdS_3 admits a class of D-branes with AdS_2 world-volume supporting an electric field [33]. Open strings stretched between two such D-branes carry a net electric charge under the difference of the respective electric fields. The result for the annulus amplitude in the Euclidean case was computed in [34], and bears a close resemblance with the heat kernel (3.6) of the magnetic Laplacian on H_2 . It would be interesting to revisit the analytic continuation to the Lorentzian case, and see whether the world-sheet duality transformation used in getting this result may shed light on the construction of a modular invariant partition function in the heterotic case.
- Finally, it would be interesting to revisit the problem originally envisaged in [20] of the pair production of charged particles in two-dimensional de Sitter space. This amounts to reversing the interpretation of the space and time coordinates of the Poincaré patch of AdS_2 , and flipping the sign of M^2 . The classical trajectories of a charged particle in dS_2 are therefore obtained by reading Figure 1 for tachyonic trajectories sideways. By analogy, we expect the upper bound on the mass of particles in dS_2 to be lowered in the presence of an electric field. It would be interesting to compute the modifications to the cosmological particle production rate due to the electric field⁹.

To conclude, we feel that a quantum analysis of electromagnetic phenomena in strongly curved space-times such as $AdS_2 \times S^2$ may be of great value for studying black hole physics or cosmology.

⁸We thank C. Bachas for pointing this out to us.

⁹This has been studied very recently at a semi-classical level including the gravitational field in [37].

Acknowledgements: It is a pleasure to thank M. Berkooz, O. Domenico, D. Israel, C. Kounnas, M. Petropoulos and M. Rozali for useful discussions, and especially C. Bachas for insightful comments on the first version of this paper.

A. Zeta function regularisation

In this appendix we discuss an alternative way to regularize the one-loop amplitude, using zeta-function regularization [20]. This will turn out to yield a different imaginary part for the one-loop amplitude, which may be interpreted as arising from a different choice of vacuum and boundary conditions.

Indeed, one may obtain the free energy from the derivative at $z = 0$ of the zeta function $\zeta_B(z)$ associated to the magnetic Laplacian,

$$W_B = -\zeta'_B(0) , \quad \zeta_B(z) := \text{Tr} (H_B + M^2)^{-z} \quad (\text{A.1})$$

Using the same manipulations as in Section 3.2, we can rewrite $\zeta_B(z)$ as a contour integral along the same contour C as in (3.10),

$$\zeta_B(z) = \frac{V}{4\pi^2 i} \int_C d\nu \nu \left[\psi \left(\frac{1}{2} + i\nu - B \right) + \psi \left(\frac{1}{2} + i\nu + B \right) \right] [w(\nu)]^{-z} \quad (\text{A.2})$$

where we defined

$$w(\nu) = \frac{1}{4} + B^2 + \nu^2 + M^2 \quad (\text{A.3})$$

As it stands however, $\zeta_B(z)$ is only well-defined for $\Re(z) > 1$. In order to continue near $z = 0$, one should subtract the leading contribution at $\nu \rightarrow \infty$: approximating $\psi(x) \sim \log x$, this is

$$\frac{V}{2\pi^2 i} \int_C d\nu \nu \log \nu [w(\nu)]^{-z} = \frac{V}{4\pi} \frac{[w(0)]^{1-z}}{z-1} \quad (\text{A.4})$$

Adding and subtracting this term, we may rewrite the heat kernel as

$$\begin{aligned} \zeta_B(z) &= \frac{V}{4\pi} \frac{[w(0)]^{1-z}}{z-1} \\ &+ \frac{V}{4\pi^2 i} \int_C d\nu \nu \left[\psi \left(\frac{1}{2} + i\nu - B \right) + \psi \left(\frac{1}{2} + i\nu + B \right) - 2 \log \nu \right] [w(\nu)]^{-z} \end{aligned} \quad (\text{A.5})$$

which converges for $\Re(z) > -1/2$, and is therefore suitable to compute the free energy (A.1).

Let us now analytically continue the euclidean result by setting $B = e^{i\theta} E$ and increasing θ from 0 to $\pi/2$. as in Section 3.2. For $\theta = 0$, in addition to the poles (3.9), there are two semi-infinite cuts along the imaginary axis, starting at $\nu = \pm i(\sqrt{w(0)} + \mathbb{R}^+)$ in the lower and upper half plane respectively. As θ is increased up to $\pi/2$, $w(\nu)$ rotates to

$$\tilde{w}(\nu) = M^2 - E^2 + \frac{1}{4} + \nu^2 \quad (\text{A.6})$$

We now split the discussion according to the sign of $\tilde{w}(0)$ (see Figure 4):

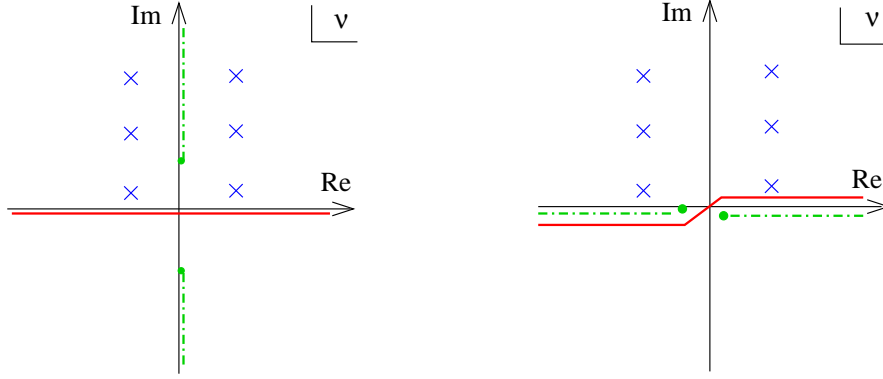


Figure 4: Analytic structure of the heat kernel and zeta function and the electric Laplacian in the ν plane, for subcritical (left) and supercritical (right) electric field. The green dotted line denotes the cut from $\log w(\nu)$.

- For $M^2 > E^2 - 1/4$ (small electric field), the cuts stay on the imaginary axis at $\nu = \pm i(\sqrt{M^2 + 1/4 - E^2} + \mathbb{R}^+)$. We can therefore move the contour C toward the real axis. Since $\tilde{w}(\nu)$ remains positive for any ν , we obtain

$$\zeta_E(z) = \frac{V}{4\pi} \frac{\tilde{w}(0)^{1-z}}{z-1} + \int_0^\infty d\nu \tilde{\rho}_E(\nu) [\tilde{w}(\nu)]^{-z} \quad (\text{A.7})$$

where $\rho_E(\nu)$ is the density of continuous states (3.17) in the electric problem, and $\tilde{\rho}_E(\nu) = \rho_E(\nu) - \nu V/(2\pi)$. The resulting free energy

$$W_E = -\zeta'_E(0) = \frac{V}{4\pi} \tilde{w}(0) (1 - \log \tilde{w}(0)) + \int_0^\infty d\nu \tilde{\rho}_E(\nu) \log \tilde{w}(\nu) \quad (\text{A.8})$$

is a real convergent integral, in agreement with the fact that there is no pair creation for small electric field.

- For $M^2 + 1/4 < E^2$ (large electric field), the cuts at $\theta = \pi/2$ migrate to the real axis at $\nu = \pm(\sqrt{E^2 - M^2 - 1/4} + \mathbb{R}^+)$ when $M^2 < E^2 - 1/4$. The contour C now runs below the real axis for $\nu < E^2 - M^2 - 1/4$, and above the real axis for $\nu \geq E^2 - M^2 - 1/4$. Noting that $\tilde{w}(\nu)$ becomes negative for $\nu \in [0, E^2 - M^2 - 1/4]$, we obtain

$$\begin{aligned} \zeta_E(z) &= \frac{V}{4\pi} \frac{e^{i\pi(1-z)} [-\tilde{w}(0)]^{1-z}}{z-1} + e^{-i\pi z} \int_0^{\sqrt{E^2 - M^2 - 1/4}} d\nu \tilde{\rho}_E(\nu) [-\tilde{w}(\nu)]^{-z} \\ &+ \int_{\sqrt{E^2 - M^2 - 1/4}}^\infty d\nu \tilde{\rho}_E(\nu) [w(z)]^{-z}. \end{aligned} \quad (\text{A.9})$$

where the (subtracted) density of states $\tilde{\rho}_E(\nu)$ is given by the same equation (3.17) as before. Computing $-\zeta'_E(0)$, we now obtain both a real and imaginary part for the

free energy,

$$\begin{aligned} \Re(W_E) &= \frac{V}{4\pi} \tilde{w}(0) (1 - \log|\tilde{w}(0)|) + \int_{\sqrt{E^2-M^2-1/4}}^{\infty} d\nu \tilde{\rho}_E(\nu) \log \tilde{w}(\nu) \\ &\quad + \int_0^{\sqrt{E^2-M^2-1/4}} d\nu \tilde{\rho}_E(\nu) \log[-\tilde{w}(\nu)] \end{aligned} \quad (\text{A.10})$$

$$\Im(W_E) = \frac{V}{4} |\tilde{w}(0)| + \pi \int_0^{\sqrt{E^2-M^2-1/4}} d\nu \tilde{\rho}_E(\nu) \quad (\text{A.11})$$

The volume term may be reabsorbed by restoring $\rho_E(\nu)$ into the integral.

As in the body of the paper, we may further process the imaginary part of the amplitude (A.11) by expanding the density of states as a difference of geometric series (3.19). Integrating term by term, we obtain

$$\begin{aligned} \Im(W_E) &= -\frac{V\Delta}{4\pi} \left[\text{Li}_1\left(-e^{-2\pi(E-\Delta)}\right) + \text{Li}_1\left(-e^{-2\pi(E+\Delta)}\right) \right] \\ &\quad + \frac{V}{8\pi^2} \left[\text{Li}_2\left(-e^{-2\pi(E-\Delta)}\right) - \text{Li}_2\left(-e^{-2\pi(E+\Delta)}\right) \right] \end{aligned} \quad (\text{A.12})$$

Similarly, for spin 1/2 fields, we obtain

$$\begin{aligned} \Im(W_{E,1/2}) &= -\frac{V\Delta_{1/2}}{2\pi} \left[\text{Li}_1\left(e^{-2\pi(E-\Delta_{1/2})}\right) + \text{Li}_1\left(e^{-2\pi(E+\Delta_{1/2})}\right) \right] \\ &\quad + \frac{V}{4\pi^2} \left[\text{Li}_2\left(e^{-2\pi(E-\Delta_{1/2})}\right) - \text{Li}_2\left(e^{-2\pi(E+\Delta_{1/2})}\right) \right] \end{aligned} \quad (\text{A.13})$$

In contrast to (3.25),(3.32), these results exhibit the contribution of two saddle points with action $2\pi(E \pm \Delta)$. Only the saddle point with action $2\pi(E - \Delta)$ has a semi-classical interpretation as a tunneling process. In the framework of the analysis of the one-loop amplitude in Section 3, the other saddle point originates from negative Schwinger time. We believe that the two results are equally valid, but for different choices of vacua and boundary conditions. An important property of the result (A.12),(A.13) is that the imaginary part of the one-loop amplitude vanishes at threshold. Applied to a supersymmetric context, this indicates that BPS particles are not emitted in this vacuum.

B. Gravitational back-reaction

In this appendix, we briefly discuss the relation of our results for pair creation in AdS_2 to the classic calculation of the neutralization of the cosmological constant by brane creation [35] (see their Appendix B for the two-dimensional case), to which we refer for many details.

Let us summarize the main results. In imaginary time, pair creation of particles in AdS_2 amounts to the nucleation of a bubble of AdS space of cosmological constant Λ_i inside an AdS space of cosmological constant Λ_o . The Euclidean instanton can be obtained by gluing two copies of H_2 , in compatibility with the Israel matching conditions. In the

semi-classical approximation, the pair production rate is proportional to e^{-S} , where S is the difference of the action of AdS with (resp. without) the bubble,

$$S = 2\pi M\bar{\rho} - \frac{4\pi}{G} \log \frac{\bar{r}_i}{\bar{r}_o} + \frac{2\pi\bar{\rho}}{G}(\Lambda_i\bar{r}_i - \Lambda_o\bar{r}_o) \quad (\text{B.1})$$

Here M is the mass of the charged particle, $\bar{\rho}$ is the classical proper radius of a particle trajectory, and G is Newton's constant. The conformal factors of the metrics of the instanton and the background are given in terms of inside and outside radii \bar{r}_i, \bar{r}_o as:

$$\bar{r}_{i,o} = \frac{2}{\Lambda_{i,o}\bar{\rho}} \left(1 - \sqrt{1 - \Lambda_{i,o}\bar{\rho}^2} \right). \quad (\text{B.2})$$

The equations of motion imply the following equations for the cosmological constants and the electric fields inside and outside the particle trajectory

$$\begin{aligned} \Lambda_{i,o} &= \lambda + \frac{G}{2}E_{i,o}^2 \\ E_o - E_i &= e \\ -(\bar{\rho}^{-2} - \Lambda_o)^{1/2} + (\bar{\rho}^{-2} - \Lambda_i)^{1/2} &= \frac{G}{2}M \\ -(\bar{\rho}^{-2} - \Lambda_o)^{1/2} - (\bar{\rho}^{-2} - \Lambda_i)^{1/2} &= -2\frac{e}{2M}(E_i + E_o), \end{aligned} \quad (\text{B.3})$$

where e is the charge of the particle and $E_{i,o}$ are the electric fields inside and outside the particle trajectories. Let us define the difference between the cosmological constants as ($E > 0$):

$$\Lambda_i - \Lambda_o = \frac{G}{2}(E_i + E_o)(E_i - E_o) \equiv -GE. \quad (\text{B.4})$$

Note that E has to be positive, since pair creation tends to reduce the cosmological constant.

In order to make contact with the semi-classical analysis in the bulk of the paper, we will set $\Lambda_o = -1/a^2 = -1$, and expand the results in terms of the gravitational coupling constant G . The quantity E is roughly the background electric field times the charge of the particle, and will coincide with our definition for the electric field E in the bulk of the paper, in the weak-gravity limit.

By extremizing the action with respect to the classical radius $\bar{\rho}$ we find:

$$\bar{\rho} = (\Lambda_o + 1/M^2(E + GM^2/4)^2)^{-1/2}. \quad (\text{B.5})$$

To obtain the particle production rate, we evaluate the action for the instanton. Expanding in powers of the gravitational coupling, we find at next-to-leading order the result in Eq. (4.3). In addition, we note that the value of our radius variable R at the extremum of the action is:

$$\frac{R}{y_0} = \frac{\bar{\rho}}{1 + \bar{\rho}^2} = \frac{M}{|E| - GM^2/4}, \quad (\text{B.6})$$

While this agrees with the value (2.34) found in the bulk of the paper at small G , it implies that the instanton exists only when

$$|E| > M + GM^2/4, \quad (\text{B.7})$$

The threshold for pair production is thus slightly raised by gravitational effects, as compared to the generalized Breitenlohner-Freedman bound (4.1). It would be interesting to extend this analysis to the case of charged BPS particles.

References

- [1] G. W. Gibbons, “Antigravitating Black Hole Solitons With Scalar Hair In N=4 Supergravity,” Nucl. Phys. B **207** (1982) 337;
G. W. Gibbons and K. i. Maeda, “Black Holes And Membranes In Higher Dimensional Theories With Dilaton Fields,” Nucl. Phys. B **298** (1988) 741;
D. Garfinkle, G. T. Horowitz and A. Strominger, “Charged Black Holes In String Theory,” Phys. Rev. D **43**, 3140 (1991) [Erratum-ibid. D **45**, 3888 (1992)].
- [2] S. Ferrara, R. Kallosh and A. Strominger, “N=2 extremal black holes,” Phys. Rev. D **52**, 5412 (1995) [arXiv:hep-th/9508072].
- [3] G. W. Moore, “Les Houches lectures on strings and arithmetic,” arXiv:hep-th/0401049.
- [4] J. M. Maldacena, J. Michelson and A. Strominger, “Anti-de Sitter fragmentation,” JHEP **9902** (1999) 011 [arXiv:hep-th/9812073].
- [5] M. Spradlin and A. Strominger, “Vacuum states for AdS(2) black holes,” JHEP **9911**, 021 (1999) [arXiv:hep-th/9904143].
- [6] W. T. Kim, “AdS(2) and quantum stability in the CGHS model,” Phys. Rev. D **60**, 024011 (1999) [arXiv:hep-th/9810055].
- [7] D. Gaiotto, A. Simons, A. Strominger and X. Yin, “D0-branes in black hole attractors,” arXiv:hep-th/0412179; D. Gaiotto, A. Strominger and X. Yin, “Superconformal black hole quantum mechanics,” arXiv:hep-th/0412322.
- [8] N. Berkovits, M. Bershadsky, T. Hauer, S. Zhukov and B. Zwiebach, “Superstring theory on AdS(2) x S(2) as a coset supermanifold,” Nucl. Phys. B **567**, 61 (2000) [arXiv:hep-th/9907200].
- [9] S. B. Giddings, J. Polchinski and A. Strominger, “Four-dimensional black holes in string theory,” Phys. Rev. D **48**, 5784 (1993) [arXiv:hep-th/9305083]; D. A. Lowe and A. Strominger, “Exact four-dimensional dyonic black holes and Bertotti-Robinson space-times in string theory,” Phys. Rev. Lett. **73**, 1468 (1994) [arXiv:hep-th/9403186].
- [10] C. V. Johnson, “Heterotic Coset Models,” Mod. Phys. Lett. A **10**, 549 (1995) [arXiv:hep-th/9409062]; P. Berglund, C. V. Johnson, S. Kachru and P. Zaugg, “Heterotic Coset Models and (0,2) String Vacua,” Nucl. Phys. B **460**, 252 (1996) [arXiv:hep-th/9509170].
- [11] D. Israel, C. Kounnas, D. Orlando and P. M. Petropoulos, “Electric / magnetic deformations of S**3 and AdS(3), and geometric cosets,” arXiv:hep-th/0405213.
- [12] A. Strominger, “AdS(2) quantum gravity and string theory,” JHEP **9901**, 007 (1999) [arXiv:hep-th/9809027].
- [13] G. W. Gibbons and P. K. Townsend, “Black holes and Calogero models,” Phys. Lett. B **454**, 187 (1999) [arXiv:hep-th/9812034].
- [14] D. M. Thompson, “AdS solutions of 2D type 0A,” arXiv:hep-th/0312156.

- [15] A. Strominger, “A matrix model for AdS(2),” *JHEP* **0403**, 066 (2004) [arXiv:hep-th/0312194].
- [16] H. Verlinde, “Superstrings on AdS(2) and superconformal matrix quantum mechanics,” arXiv:hep-th/0403024.
- [17] E. D’Hoker, D. Z. Freedman and R. Jackiw, “SO(2,1) Invariant Quantization Of The Liouville Theory,” *Phys. Rev. D* **28**, 2583 (1983).
- [18] D. Brill, “Splitting of an extremal Reissner-Nordstrom throat via quantum tunneling,” *Phys. Rev. D* **46**, 1560 (1992) [arXiv:hep-th/9202037].
- [19] R. Britto-Pacumio, J. Michelson, A. Strominger and A. Volovich, “Lectures on superconformal quantum mechanics and multi-black hole moduli arXiv:hep-th/9911066.
- [20] A. Comtet and P. J. Houston, “Effective Action On The Hyperbolic Plane In A Constant External Field,” *J. Math. Phys.* **26**, 185 (1985).
- [21] T. Nakatsu and N. Yokoi, ‘Comments on Hamiltonian formalism of AdS/CFT correspondence,” *Mod. Phys. Lett. A* **14**, 147 (1999) [arXiv:hep-th/9812047].
- [22] E. Brezin and C. Itzykson, “Pair Production In Vacuum By An Alternating Field,” *Phys. Rev. D* **2** (1970) 1191.
- [23] M. Berkooz, and B. Pioline, “Strings in an electric field, and the Milne universe,” *JCAP* **0311** (2003) 007 [arXiv:hep-th/0307280].
- [24] A. Comtet, “On The Landau Levels On The Hyperbolic Plane,” *Annals Phys.* **173** (1987) 185.
- [25] C. Grosche, “Path Integration On The Hyperbolic Plane With A Magnetic Field,” *Annals Phys.* **201** (1990) 258.
- [26] M. Antoine, A. Comtet and S. Ouvry, “Scattering On An Hyperbolic Torus In A Constant Magnetic Field,” *J. Phys. A* **23** (1990) 3699.
- [27] U. H. Danielsson, E. Keski-Vakkuri and M. Kruczenski, “Vacua, propagators, and holographic probes in AdS/CFT,” *JHEP* **9901** (1999) 002 [arXiv:hep-th/9812007].
- [28] I. K. Affleck, O. Alvarez and N. S. Manton, “Pair Production At Strong Coupling In Weak External Fields,” *Nucl. Phys. B* **197**, 509 (1982); I. K. Affleck and N. S. Manton, “Monopole Pair Production In A Magnetic Field,” *Nucl. Phys. B* **194**, 38 (1982).
- [29] M. Berkooz, B. Pioline and M. Rozali, “Closed strings in Misner space: Cosmological production of winding strings,” *JCAP* **0408**, 004 (2004) [arXiv:hep-th/0405126].
- [30] P. Breitenlohner and D. Z. Freedman, “Stability In Gauged Extended Supergravity,” *Annals Phys.* **144** (1982) 249.
- [31] J. S. Schwinger, “On Gauge Invariance And Vacuum Polarization,” *Phys. Rev.* **82** (1951) 664.
- [32] N. Marcus, “Unitarity And Regularized Divergences In String Amplitudes,” *Phys. Lett. B* **219**, 265 (1989).
- [33] C. Bachas and M. Petropoulos, “Anti-de-Sitter D-branes,” *JHEP* **0102**, 025 (2001) [arXiv:hep-th/0012234].

- [34] P. Lee, H. Ooguri and J. w. Park, “Boundary states for AdS(2) branes in AdS(3),” Nucl. Phys. B **632** (2002) 283 [arXiv:hep-th/0112188]; B. Ponsot, V. Schomerus and J. Teschner, “Branes in the Euclidean AdS(3),” JHEP **0202**, 016 (2002) [arXiv:hep-th/0112198]; S. Ribault, “Two AdS(2) branes in the Euclidean AdS(3),” JHEP **0305**, 003 (2003) [arXiv:hep-th/0210248].
- [35] J. D. Brown and C. Teitelboim, “Neutralization Of The Cosmological Constant By Membrane Creation,” Nucl. Phys. B **297** (1988) 787.
- [36] C. Teitelboim, “Gravitation And Hamiltonian Structure In Two Space-Time Dimensions,” Phys. Lett. B **126**, 41 (1983).
- [37] A. Gomberoff, M. Henneaux and C. Teitelboim, “Decay of the Cosmological Constant. Equivalence of Quantum Tunneling and Thermal Activation in Two Spacetime Dimensions”, arXiv:hep-th/0501152.